Corrective Osteotomies of Phalangeal and Metacarpal Malunions Using Patient-Specific Guides: CT-Based Evaluation of the Reduction Accuracy

Hirsiger, Stefanie; Schweizer, Andreas; Miyake, Junichi; Nagy, Ladislav; Fürnstahl, Philipp

Abstract: BACKGROUND Surgical planning of corrective osteotomies is traditionally based on conventional radiographs and clinical findings. In the past 10 years, 3-dimensional (3D) preoperative planning approaches with patient-specific guides have been developed. However, the application of this technology to posttraumatic deformities of the metacarpals and phalangeal bones has not yet been investigated. Our goal was to evaluate the feasibility of the surgical application to the latter and to evaluate the extent and precision of correction. METHODS We present results of 6 patients (8 osteotomies) treated with phalangeal or metacarpal corrective osteotomy. Deformities were located in the third ray in 1, fourth ray in 3, and fifth ray in 4 cases. Six malunited metacarpal bones (1 intra-articular) and 2 deformed proximal phalanges were treated. Computer-based 3D preoperative planning using the contralateral hand as a template allowed the production of 3D-printed patient-specific guides that were used intraoperatively for navigation. The precision of the reduction was assessed using pre- and postoperative computed tomography by comparing the postoperative bone model with the preoperatively simulated osteotomy. Range of motion and grip strength were documented pre- and postoperatively. RESULTS The mean follow-up time was 6 months (range: 5-11 months). Rotational deformity was reduced from a mean of 10.0° (range: 7.2°-19.3°) preoperatively to 2.3° (range: 0.7°-3.7°) postoperatively, and translational incongruency decreased from a mean of 1.4 mm (range: 0.7-2.8 mm) to 0.4 mm (range: 0.1-0.9 mm). CONCLUSION Preliminary results indicate that a precise reduction for corrective osteotomies of metacarpal and phalangeal bones can be achieved by using 3D planning and patient-specific guides.

Corrective Osteotomies of Phalangeal and Metacarpal Malunions Using Patient-Specific Guides: CT-Based Evaluation of the Reduction Accuracy

Stefanie Hirsiger[1], Andreas Schweizer[1], Junichi Miyake[2],
Ladislav Nagy[1], and Philipp Fürnstahl[1]

Abstract

Background: Surgical planning of corrective osteotomies is traditionally based on conventional radiographs and clinical findings. In the past 10 years, 3-dimensional (3D) preoperative planning approaches with patient-specific guides have been developed. However, the application of this technology to posttraumatic deformities of the metacarpals and phalangeal bones has not yet been investigated. Our goal was to evaluate the feasibility of the surgical application to the latter and to evaluate the extent and precision of correction. **Methods:** We present results of 6 patients (8 osteotomies) treated with phalangeal or metacarpal corrective osteotomy. Deformities were located in the third ray in 1, fourth ray in 3, and fifth ray in 4 cases. Six malunited metacarpal bones (1 intra-articular) and 2 deformed proximal phalanges were treated. Computer-based 3D preoperative planning using the contralateral hand as a template allowed the production of 3D-printed patient-specific guides that were used intraoperatively for navigation. The precision of the reduction was assessed using pre- and postoperative computed tomography by comparing the postoperative bone model with the preoperatively simulated osteotomy. Range of motion and grip strength were documented pre- and postoperatively. **Results:** The mean follow-up time was 6 months (range: 5-11 months). Rotational deformity was reduced from a mean of 10.0° (range: 7.2°-19.3°) preoperatively to 2.3° (range: 0.7°-3.7°) postoperatively, and translational incongruency decreased from a mean of 1.4 mm (range: 0.7-2.8 mm) to 0.4 mm (range: 0.1-0.9 mm). **Conclusion:** Preliminary results indicate that a precise reduction for corrective osteotomies of metacarpal and phalangeal bones can be achieved by using 3D planning and patient-specific guides.

Keywords: corrective osteotomy, rapid prototyping, patient-specific guides, hand malunion, accuracy analysis

Introduction

Symptomatic malunions of the hand phalangeal and metacarpal bones are relatively rare. Whereas sagittal deformity is usually well accepted, especially in metacarpals, rotation deformity can lead to significant scissoring of fingers.[3,19,33] As no consensus about the acceptable limits of deformity exists, indication for surgical correction is usually based on clinical findings and following the subjective functional limitation of the patient.[5,10,13] The goal of surgical correction is the restoration of clinical function by correcting the anatomy. Different techniques for corrective osteotomies of metacarpal shaft malunions have been described,[13,17,46] but the correction is mostly performed at the apex of the deformity. However, for the correction of phalangeal malunions, it is debated whether an extra-anatomic metacarpal or an anatomic phalangeal osteotomy should be performed, and whether intra-articular malunions should be corrected intra- or extra-articularly.[3,7,14,40,44] Available literature about metacarpal and phalangeal corrective osteotomies mainly consists of reports on small cohorts analyzed retrospectively.[13] Satisfactory outcomes in terms of precision of the reduction and improvement of hand function have been described for osteotomies based on conventional x-ray.[5,7,30,44] Although plain radiographs still remain the standard for assessing bone deformities, 3-dimensional (3D) computed tomography (CT) imaging permits a more exact assessment of the deformity in space that cannot be

[1]University of Zurich, Switzerland
[2]Osaka University, Japan

Supplemental material is available in the online version of the article.

Corresponding Author:
Philipp Fürnstahl, Department of Orthopedics, University Hospital Balgrist, University of Zurich, Forchstrasse 340, Zürich 8008, Switzerland.
Email: philipp.fuernstahl@card.balgrist.ch

obtained by conventional radiographs or 2-dimentional CT images.[26] Particularly, 3D bone models can be generated from CT and used for a more precise deformity analysis and the subsequent computer-based simulation of the corrective osteotomy. Recent advances in 3D-printing technology have facilitated production of patient-specific guides, enabling transfer of the computer-based planning onto the intraoperative site. This approach has been successfully applied for the upper extremity, particularly for performing corrective osteotomies of the forearm bones.[11,24,25,28,36,38,42]

Surprisingly, very few studies have analyzed the surgical outcome with postoperative CT data,[21,29,43] and only 1 study has compared the outcome of conventional versus 3D-planned corrections.[43] It was shown that more anatomic correction of scaphoid malunions was obtained by using patient-specific guides.[39] We applied the technology of 3D-planned patient-specific guides to malunions of metacarpals and phalanges. Our goal was to evaluate the feasibility of the application to small and smooth-surfaced bones through relatively small approaches and to evaluate the extent and precision of correction. We report our experience of treating 6 patients (8 osteotomies) with phalangeal or metacarpal corrective osteotomy using computer-based 3D planning preoperatively and 3D-printed patient-specific guides intraoperatively.

Methods

Data Acquisition

Between 2012 and 2014, 6 patients were treated by extra- (7 cases) or intra-articular (1 case) corrective osteotomies of a metacarpal (6 cases) or phalangeal (2 cases) bone using 3D preoperative planning and patient-specific guides.

Inclusion criterion was the presence of an objectivated metacarpal or phalangeal posttraumatic deformity that was symptomatic to an extent where the patient wished surgical correction. Exclusion criteria were pregnancy (impossibility of CT scans) and refusal to participate in the study.

Approval of the responsible ethical committee and informed patient consent were obtained. Preoperatively, CT scans of the affected and the contralateral hand were acquired. Six to 8 weeks postoperatively, an additional CT scan of the operated bone was performed. The data were acquired with an axial resolution of 0.67 mm using a Philips Brilliance 40 CT device (Philips, Best, the Netherlands).

3D Preoperative Planning

The CT data of the pathological and contralateral healthy bone were segmented using commercially available software and converted to 3D triangular surface models (Mimics; Materialise, Leuven, Belgium). Thereafter, the 3D models were imported into the preoperative planning software CASPA (Balgrist Card AG, Zurich, Switzerland).

Following the template-based approach described for osteotomies of the forearm,[11,37,38,42] the contralateral bone model was used as a reconstruction template for the quantification of the malunion and, subsequently, for the simulation of the osteotomy. The transformation of the fragments was expressed relative to an anatomical coordinate system, which was created and aligned to the bone such that the x-axis corresponds to the volar-dorsal and the y-axis to the longitudinal axis of the bone, as described by Wu et al.[45] The 3D models of the deformed bone (Figure 1a) and the mirrored contralateral reference bone (Figure 1b) were then proximally aligned (Figure 1c) using the Iterative Closest Point (ICP) surface registration method.[6] Next, the osteotomy and reduction were simulated. The deformed bone model was cut and the distal bone fragment was aligned to the contralateral mirrored reference template (Figure 1d). The relative transformation between the 2 positions of the distal bone fragments pre and post alignment represents the degree of deformity and, consequently, the amount of the required correction.[36]

In the presented case series, different types of osteotomy were required to correct the deformity (see Table 1). For simple wedge osteotomies (3 cases), the osteotomy planes were defined manually at the apex of the deformity and normal to the bone length axis. If no shortening existed, a so-called crossing osteotomy can be planned (see Supplemental Material 1, clinical case 2a and 2b). The latter consists of a partial opening and closing osteotomy with 2 osteotomy planes that intersect at the center of the bone. The benefit of a crossing osteotomy is that less shortening of the bone results compared to a closing wedge osteotomy and that a smaller gap is created than in an opening wedge osteotomy. Another benefit is that the cutting waste resulting from the closing part can be used to fill the gap of the opening part.

For the cases where a multiplanar deformity with a dominating rotational component was present, a so-called single-cut osteotomy was calculated (clinical case 5 and 6b). In this type of osteotomy, the 3D correction can be achieved by sliding and rotating in 1 single plane, thus not creating any gaps. This optimal plane can be found mathematically, using technical devices or by computed simulation.[11,23] Last, 2 or more planar cuts can be combined for correction of multifragmentary extra- and intra-articular deformities (see Supplemental Material 2, clinical case 4).

After simulation of the osteotomy and reduction as described above, the patient-specific guides were designed using the CASPA software. The basic principle of the guide design is that a guide body is molded to the bone surface such that it can be placed on its specifically planned position intraoperatively. To aid the final reduction, guides for predrilling screw holes, additional reduction guides, or a combination of both were used.[11,42] In a first step, a model of the implant (ie, 1.5-mm locking compression plate;
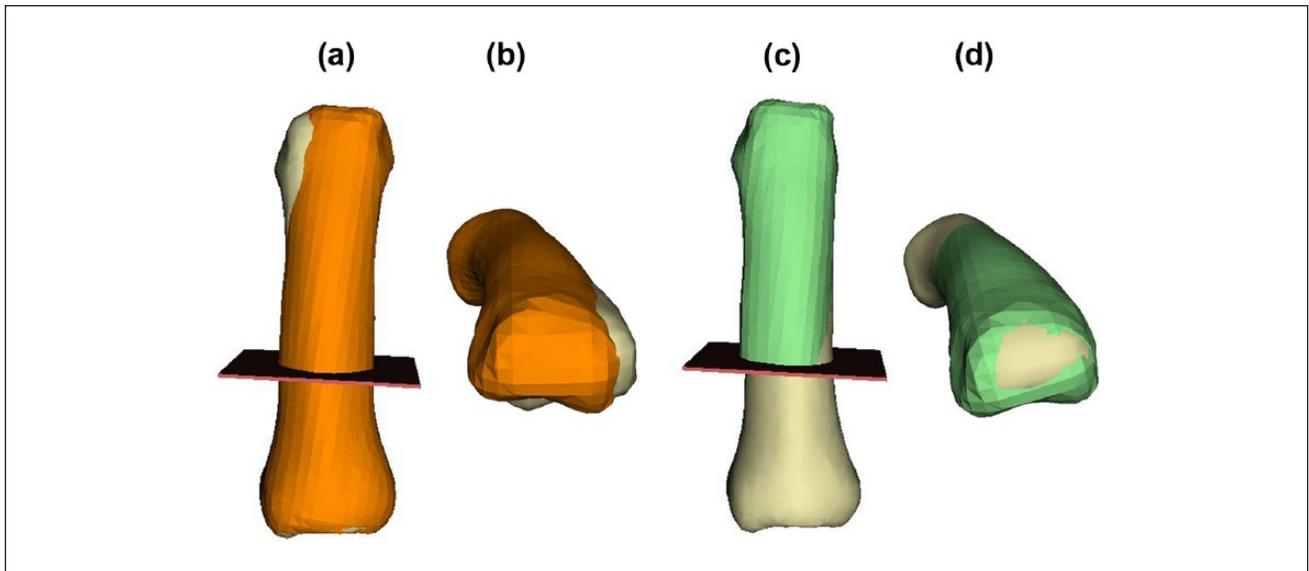
Figure 1. First, the deformed bone (left) and mirrored contralateral healthy template (right) were matched, hereby aligning the proximal part (a), rotational deformity visible in axial view (b). The pathologic bone was then osteotomized digitally and the distal part was aligned to the template. Planned correction in a dorsoventral view (c) and axial view (d).

Synthes DePuy, New Brunswick, New Jersey) was positioned on the reduced bone surface (Figure 2a). The angular-stable locking screws of the implant were modeled as cylinder objects (Figure 2b). The screw holes were then transformed back to the pathologic position by applying the inverse reduction (Figure 2c), a technique described previously.[1,42] Based on the back-transformed position, a prereduction drilling guide was designed to prepare the holes for the angular-stable locking screws using K-wires (Figure 2d). The proximal guide part included a planar surface, which acted as a cutting jig (Figure 2e). By using this technique, the drill holes can be placed in the uncut bone in the malunited position. Once the osteotomy is made, the application of the angular-stable implant and usage of the prepared drill holes as screw holes will reduce the fragment to the planned position and correct the deformity.

The guides were manufactured by Medacta SA (Castel San Pietro, Switzerland) using a 3D printer (ie, selective laser sintering device) and biocompatible polyamide 1PA 2200. The guides were sterilized using conventional steam pressure.

Surgical Technique

The surgeries were performed by 2 senior hand surgeons (A.S., L.N.). The approach was chosen dependent upon the location of the deformity. For all but 2 cases, a dorsal approach was used and the extensor mechanism was split (case 2: intermetacarpal approach for correction of metacarpal IV and V, and case 4: ulnar approach for intra-articular metacarpal V correction).

Case 6 is presented to demonstrate the surgical technique (Figure 3). The malunion of the fourth ray consisted of a flexion deformity of the metacarpal, and additionally, a rotational deformity of the phalanx was present (Figure 3a). The bone was exposed subperiosteally in the area where the prereduction guide has to be placed. Thereafter, the guide was fixed to the bone using two 1.0-mm K-wires and the screw holes of the implant were predrilled using four 1.5-mm K-wires (Figure 3b), 2 each into the proximal and distal parts. Next, a guided osteotomy was performed with an oscillating saw (Figure 3c). The implant was fixed to the bone using the predrilled screw holes. By doing so, the fragments were reduced to the plate as planned, in this case supported by an additional reduction guide (Figure 3d).

In case of opening wedge osteotomies, bone defects were filled with autologous cancellous bone obtained from the radius through a dorsal approach over the Lister tubercle. Whenever possible, the periosteum was adapted over the plate. The extensor mechanism and skin were sutured.

Postoperative Evaluation

Patients were regularly seen for postoperative follow-up examinations. Six to 12 weeks after surgery, a clinical and radiological examination was performed in which a CT scan of the operated hand was acquired. For clinical evaluation, grip strength using a dynamometer (Jamar; Smith and Nephew, Memphis, Tennessee) and range of motion of the 3 metacarpophalangeal and interphalangeal joints were obtained. Range of motion was expressed as combined value for all 3 joints.[19] The patients were asked to

Table 1. Demographic and Surgical Patient Data.

Patient No.	Age (years)	Affected bone	Side	Initial treatment	Clinical deformity	Interval injury—OT (months)	Implant	Type of OT	Graft	Follow-up (months)	Reoperation	Level of satisfaction
1	34	5. Metacarpal (subcapital)	R	K-wire	Flexion	9	2.0 LCP-condyle 4 holes	Opening wedge + Capsulotomy Metacarpal V	Local (resection)	6	—	S.
2a	28	4. Metacarpal (epibasal)	R	K-wire	Flexion and Malrotation	8	2.0 LCP-condyle 3 holes	Crossing wedge + Recentering of extensor apparatus	Spongious radius bone graft (lister)	7	—	S.
2b		5. Metacarpal (subcapital)	R	Conservative	Flexion	8	2.0 LCP 4 holes	Crossing wedge	Spongious radius bone graft (lister)	7	—	S.
3	15	5. Phalanx (epibasal)	L	Conservative	Ulnar deviation, Extension	6	1.5 condyle 3 holes	Opening wedge	Corticospongious radius bone graft (lister)	10	Plate removal after 9 months	V.S.
4	26	5. Metacarpal (base)	R	Conservative	Intra-articular malunion, Flexion	7	2.0 LCP-condyle plate 4 holes	Intra-articular multifragment and extra-articular complex	Spongious radius bone graft (lister)	11	Plate removal after 4 months	S.
5	51	3. Metacarpal (shaft)	L	Conservative	Ulnar deviation, Rotation	14	2.0 LCP-condyle rotation corr. 4 holes	Single cut	None	5	—	V.S.
6a	21	4. Metacarpal (shaft)	R	Conservative	Flexion	60	2.4 LCP 4 holes	Opening wedge + nerve readaption	Corticospongious radius bone graft (lister)	5	—	V.S.
6b		4. Phalanx (shaft)	R	Conservative	Malrotation	85	1.5 LCP-condyle plate 4 holes	Single cut	None	5		V.S.

Note. OT= osteotomy; R = right; L = left; K-wire = Kirschner wire; LCP = locking compression plate; V.S. = very satisfied; S. = satisfied.
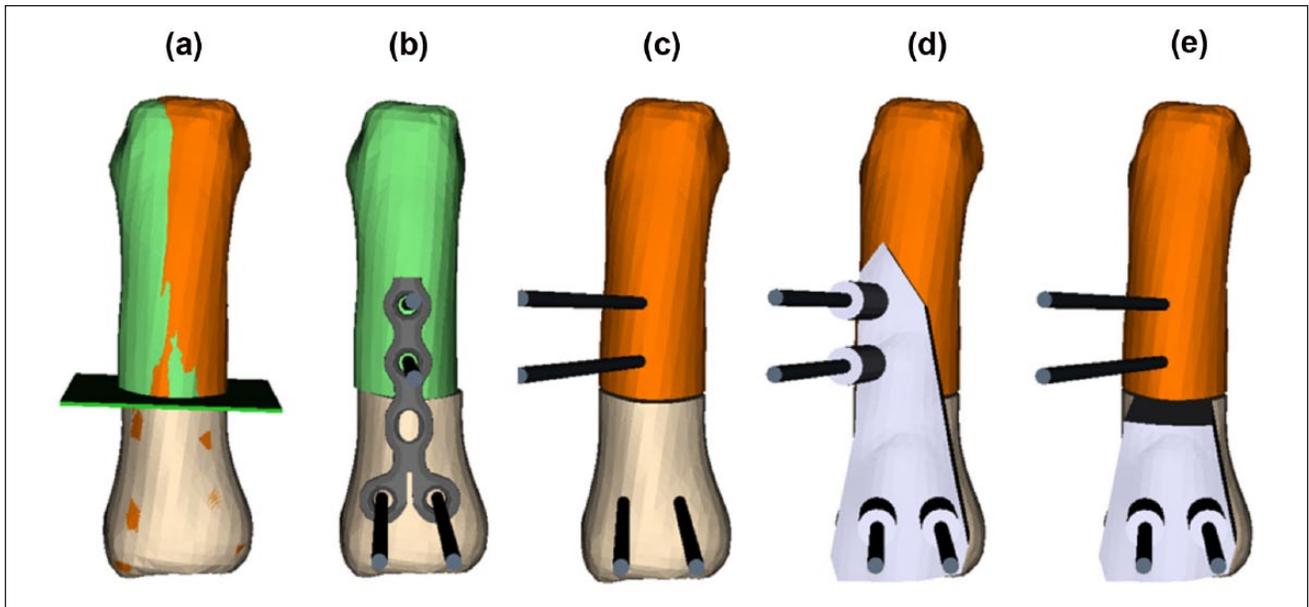
Figure 2. Planned correction (left) and pathologic bone (right) (a). Planned correction with plate and K-wires for screw holes (b). Inverse transformation back to the pathologic position (c). Construction of the guide (d). Proximal guide part serves as cutting jig (e).

rate the result subjectively (not satisfied, satisfied, or very satisfied).

The postoperative CT was used for comparing the preoperative plan with the surgical outcome. A 3D model of the corrected bone was generated by applying the same segmentation method as for the preoperative planning (see Supplemental Material 3). The metal implant was digitally subtracted from the CT data by eliminating the respective density values using global thresholding. Remaining metal artifacts of osteosynthesis material were removed manually from the segmentation result. The bone fragments proximal to the osteotomy were used as a common reference and registered using ICP (Supplemental Material 3b). Thereafter, the difference between planned and performed reduction was measured by computing the difference between the distal bone fragments using ICP. The difference between the 2 positions of the distal fragment was expressed by 3 rotations around (described by 3 Euler rotations[35]) and 3 translations along the previously established coordinate system. To compare the residual deformity error between cases, single values for the rotation and translation were calculated. 3D rotational error was measured in axis-angle representation (hereinafter 3D angle).[35] The residual displacement was expressed as the Euclidean length of the 3D displacement vector (hereinafter 3D translation).

Results

Demographic data and details about the surgical approach are summarized in Table 1. All patients were male and had an average age of 30.7 years (range: 14-73 years) at the time of the surgery. Deformities were located in the third ray in 1, fourth ray in 3, and fifth ray in 4 cases. Six malunited metacarpal bones and 2 deformed proximal phalanges were treated. All fractures were initially treated in other institutions, 2 by percutaneous pinning, and 6 conservatively.

Five deformities were treated by wedge osteotomies, 1 by a combined intra- and extra-articular osteotomy, and 2 by single-cut osteotomies. The mean follow-up time was 6 months (range: 5-11 months). Within this time, 2 patients required implant removal due to local soft-tissue irritation. No other postoperative complications were observed. There was no implant failure or delayed healing visible on the postoperative CT scans, all osteotomies went to union. All patients were satisfied or very satisfied with the result.

Results of the pre- and postoperative range of motion and grip strength measurements are given in Table 2. The combined range of motion in 3 joints (ie, metacarpophalangeal, proximal interphalangeal, and distal interphalangeal) showed a mean increase of 30° (+30° to +70°). Grip strength improved for all but 1 patient, the mean increase being 7 kg (−11 to +26 kg).

The results of the 3D deformity evaluation based on pre- and postoperative CT are presented in Tables 3 to 5. In Table 3, the preoperative deformity assessment and the precision of the reduction are given for each case with respect to 3D angle and 3D translation. In Tables 4 and 5, the same measurements were expressed according to the established coordinate system, with respect to the 3 anatomical planes.
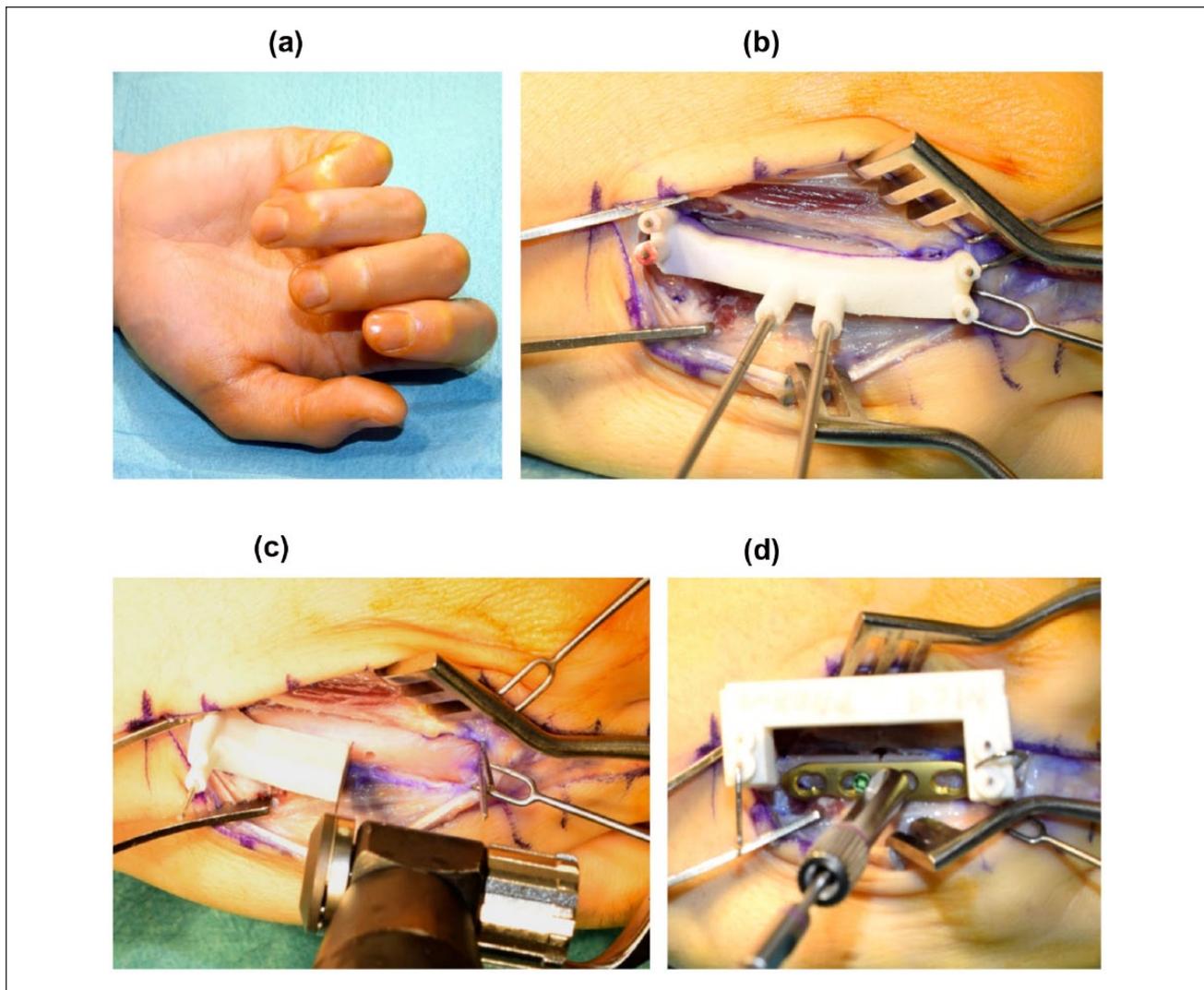
Figure 3. Intraoperative photographs showing clinical deformity (a), guide-fixation and predrilling of screw holes using K-wires (b), guided osteotomy (c) and reduction guide (d).

Table 2. Pre- and Postoperative Range of Motion and Grip Strength Measurements.

	Preoperative					Postoperative				
	ROM F/E			Grip power		ROM F/E			Grip power	
Patient No.	MP	PIP	DIP	Affected	Normal	MP	PIP	DIP	Affected	Normal
1	60/0/0	80/10/0	60/5/0	4	52	90/0/0	100/5/0	70/0/0	30	80
2a	Normal	Normal	Normal	31	45	90/0/5	Normal	Normal	36	42
2b	Normal	Normal	Normal	31	45	95/0/30	Normal	Normal	36	42
3	90/5/0	100/0/20	80/10/0	24	42	90/0/10	95/0/15	90/0/5	46	52
4	Normal	Normal	Normal	40	40	90/0/0	Normal	Normal	40	50
5	Normal	Normal	Normal	36	42	110/0/10	80/0/0	80/0/0	36	52
6a	90/10/0	100/5/0	85/5/0	45	48	90/0/0	120/0/0	110/0/0	34	43
6b	90/10/0	100/5/0	85/5/0	45	48	90/0/0	120/0/0	110/0/0	34	43

Note. ROM = range of motion; F/E = flexion/extension; MP = metacarpophalangeal joint; PIP = proximal interphalangeal joint; DIP = distal interphalangeal joint.

Table 3. Pre- and Postoperative 3D Deformity.

	Preoperative		Postoperative	
Patient No.	3D angle (degree)	3D translation (millimeter)	3D angle (degree)	3D translation (millimeter)
I	9.5	2.2	2.4	0.5
2a	7.2	0.9	1.1	0.3
2b	19.3	1.1	3.7	0.7
3	8.8	1.4	2.9	0.1
4	8.0	2.8	1.2	0.2
5	8.6	1.0	0.7	0.2
6a	8.1	0.7	3.6	0.9
6b	10.4	0.8	2.5	0.4

The mean preoperative rotational (3D angle) and translational (3D translation) deformity was 10.0° (range: 7.2°-19.3°) and 1.4 mm (range: 0.7-2.8 mm), respectively. In radial/ulnar, flexion/extension, and pro/supination direction, malrotations of 1.3° (range: 0.2°-3.0°), 6.1° (range: 3°-17.6°), and 5.9° (range: 0.7°-10.1°) were measured, respectively.

The mean residual postoperative 3D-angle and 3D-translation values were 2.3° (range: 0.7°-3.7°) and 0.4 mm (range: 0.1-0.9 mm), respectively. Residual malrotation in radial/ulnar, flexion/extension, and pro/supination direction after surgery was 0.4° (0.0°-1.8°), 0.8° (0.0°-3.5°), and 1.8° (0.6°-3.1°), respectively.

Discussion

Conventional radiographs remain the standard for initial radiologic assessment of bone deformity and thus malunions, but provide only limited precision.[5,7,30,44] Technical developments have lead to wide disponibility of CT scans, which allow more detailed evaluation of deformity.[9,26,43] The development of selective laser sintering allowed the creation of 3D models based on CT data, initial reports of the use for surgical planning date from 2 decades ago.[2] The accuracy of these techniques has subsequently been tested for dental implant placement in vitro[34] and in vivo.[8] Around the same time, the use of bone models built using rapid prototyping for preoperative planning was described for intra- and extra-articular fractures, malunions, and pedicle screw positioning.[4] First experiences with personalized drilling guides for spinal screw positioning[12,32] and wires in hip surface replacement[31] were published. Further development allowed clinical application of custom acetabular components[15,18] and patient-specific guides in prosthetic knee replacement.[22,27] The technique was adapted for the planning and execution of correction osteotomies of long bones in the upper extremity[9,16,20,25] and osteotomies around the knee[41] with promising results. The application was then extended to intra-articular correction osteotomies of the distal radius.[20,28,38] Recently, the technique has been showed to improve anatomic reduction in scaphoid reconstruction.[39] The technique has not yet been described for the correction of metacarpal and phalangeal malunions. The aim of this study was to evaluate the feasibility and precision of corrective osteotomies in metacarpal and phalangeal bones using a 3D-approach and patient-specific guides. We suspected that the very limited surgical workspace with small guide-bone contact surface and the nondistinct surface of metacarpal and phalangeal bone could negatively influence the accuracy of reduction and thus deformity correction. The small bone fragments could be in danger of osteonecrosis or nonunion and soft-tissue adhesion could limit postoperative outcome.[19] To reduce these risks, extra-anatomical correction of intra-articular and phalangeal malunions has been advocated in the past.[3] This goal is achieved by performing osteotomies more proximally, outside the zone of initial trauma. The disadvantage is the obligatory nonanatomic result.

In the presented cases of posttraumatic deformities, the technique of anatomic correction using patient-specific guides showed high precision to restore anatomy. Although we performed all corrections at the apex of deformity with concomitant soft-tissue release in 2 patients, we did not observe delayed union or fragment necrosis. Clinical evaluation showed no impairment of postoperative mobility and good patient satisfaction. These findings suggest that osteotomies of phalangeal and metacarpal bones using patient-specific guides can be performed through standard incisions and that good guide fit can be obtained despite the smooth and limited contact surface. In line with others we are convinced, that anatomic reconstruction will lead to the most physiologic result and should be the goal of a correction osteotomy.[19,30] If limiting soft-tissue adhesions are present, tendon adhesiolysis or capsulotomy can be conducted in the context of the corrective osteotomy. The presented technique is more costly and resource-intensive compared with standard techniques based on conventional radiographs. The time consumption for planning varies accordingly to the complexity of the case and can range from 2 to 4 hours with an obvious learning curve. The cost for guide manufacturing of $220 to $320[38] rises to about $2000 per case if 3D planning and guide engineering are included.

Limitations of this study include the retrospective analysis and the small sample size, the lack of a control group and lack of functional outcome scores. Consequently, the question whether the application of the presented technique is superior to conventional planning and thus indicated in all cases of corrective osteotomy cannot yet be answered with our data.

We conclude that the presented technique permits very precise correction of multiplanar deformities of metacarpal and phalangeal bones through standard surgical approaches. In our experience, 3D planning and patient-specific rapid-prototyped guides allow a detailed deformity analysis and

Table 4. Pre- and Postoperative Angulation Deformity (in Degree).

Patient No.	Preoperative			Postoperative		
	Radial + Ulnar −	Flexion + Extension −	Pronation + Supination −	Radial + Ulnar −	Flexion + Extension −	Pronation + Supination −
I	0.2	2	9.3	0.5	0.2	2.3
2a	2.3	3.4	5.8	0.3	0.5	0.9
2b	−3	17.6	−6.8	1.8	−0.9	3.1
3	−0.2	−8.7	1.4	0.3	−0.4	2.9
4	−0.2	6.4	4.8	0	0.5	1.1
5	−1.5	2.5	8.1	−0.2	−0.3	0.6
6a	−0.6	8	−0.7	−0.1	−3.5	−0.7
6b	2.5	−0.3	−10.1	−0.1	0	2.5

Table 5. Pre- and Postoperative Translation Deformity (in mm).

Patient No.	Preoperative			Postoperative		
	Radial + Ulnar −	Palmar + Dorsal −	Shortening + Lengthening −	Radial + Ulnar −	Palmar + Dorsal −	Shortening + Lengthening −
I	−0.6	0.7	2	0.4	0.2	0.1
2a	0.2	0.9	0	0.1	0.1	0.3
2b	0.2	−0.9	0.6	−0.7	0.1	0
3	0	−1.1	0.8	0.1	0.1	0
4	−0.3	−0.6	2.7	0	−0.1	0.2
5	−0.8	0.5	0.4	−0.1	−0.1	0.2
6a	−0.1	0.2	0.7	0.2	0.3	−0.8
6b	0.8	−0.2	−0.1	0	0.2	0.3

an exact correction of deformity as well as surgeon-friendly intraoperative application. While planning and correction based on standard radiographs can probably be more cost- and time-effective in simple corrections, the presented technique allows reliable and exact correction also in complex 3D deformities.

Although the results of the study are promising, a larger clinical trial with a control group must be carried out to evaluate the superiority compared with conventional planning.

Ethical Approval

This study was approved by our institutional review board.

Statement of Human and Animal Rights

All procedures followed were in accordance with the ethical standards of the responsible committee on human experimentation (institutional and national) and with the Helsinki Declaration of 1975, as revised in 2008.

Statement of Informed Consent

Informed consent was obtained from all patients for being included in the study.

References

1. Athwal GS, Ellis RE, Small CF, Pichora DR. Computer-assisted distal radius osteotomy. *J Hand Surg Am*. Nov 2003;28(6):951-958.
2. Berry E, Brown JM, Connell M, et al. Preliminary experience with medical applications of rapid prototyping by selective laser sintering. *Med Eng Phys*. 1997;19(1):90-96.

3. Bindra RR, Burke FD. Metacarpal osteotomy for correction of acquired phalangeal rotational deformity. *J Hand Surg Am*. 2009;34(10):1895-1899.

4. Brown GA, Firoozbakhsh K, DeCoster TA, Reyna JR Jr, Moneim M. Rapid prototyping: the future of trauma surgery? *J Bone Joint Surg Am*. 2003;85-A(Suppl 4):49-55.

5. Buchler U, Gupta A, Ruf S. Corrective osteotomy for post-traumatic malunion of the phalanges in the hand. *J Hand Surg Br*. 1996;21(1):33-42.

6. Chen YM, Gérard. Object modeling by registration of multiple range images. In: Proceedings of the 1991 IEEE, International Conference on Robotics and Automation; April 1991; Sacramento, CA.

7. Del Pinal F, Garcia-Bernal FJ, Delgado J, Sanmartin M, Regalado J. Results of osteotomy, open reduction, and internal fixation for late-presenting malunited intra-articular fractures of the base of the middle phalanx. *J Hand Surg Am*. 2005;30(5):1039 e1031-1039 e1014.

8. Di Giacomo GA, Cury PR, de Araujo NS, Sendyk WR, Sendyk CL. Clinical application of stereolithographic surgical guides for implant placement: preliminary results. *J Periodontol*. 2005;76(4):503-507.

9. Dobbe JG, Strackee SD, Schreurs AW, et al. Computer-assisted planning and navigation for corrective distal radius osteotomy, based on pre- and intraoperative imaging. *IEEE Trans Biomed Eng*. Jan 2011;58(1):182-190.

10. Flatt AE. Closed and open fractures of the hand. Fundamentals of management. *Postgrad Med*. 1966;39(1):17-26.

11. Fürnstahl P, Schweizer A, Graf M, et al. Surgical treatment of long-bone deformities: 3D preoperative planning and patient-specific instrumentation. In: Zheng G., Li S. (eds), *Computational Radiology for Orthopaedic Interventions*. Springer; 2016;123-149.

12. Goffin J, Van Brussel K, Martens K, Vander Sloten J, Van Audekercke R, Smet MH. Three-dimensional computed tomography-based, personalized drill guide for posterior cervical stabilization at C1-C2. *Spine*. 2001;26(12):1343-1347.

13. Gollamudi S, Jones WA. Corrective osteotomy of malunited fractures of phalanges and metacarpals. *J Hand Surg Br*. 2000;25(5):439-441.

14. Harness NG, Chen A, Jupiter JB. Extra-articular osteotomy for malunited unicondylar fractures of the proximal phalanx. *J Hand Surg Am*. 2005;30(3):566-572.

15. Holt GE, Dennis DA. Use of custom triflanged acetabular components in revision total hip arthroplasty. *Clin Orthop Relat Res*. 2004;(429):209-214.

16. Honigmann P, Thieringer F, Steiger R, Haefeli M, Schumacher R, Henning J. A simple 3-dimensional printed aid for a corrective palmar opening wedge osteotomy of the distal radius. *J Hand Surg Am*. 2016;41(3):464-469.

17. Jawa A, Zucchini M, Lauri G, Jupiter J. Modified step-cut osteotomy for metacarpal and phalangeal rotational deformity. *J Hand Surg Am*. 2009;34(2):335-340.

18. Joshi AB, Lee J, Christensen C. Results for a custom acetabular component for acetabular deficiency. *J Arthroplasty*. 2002;17(5):643-648.

19. Jupiter JB, Goldfarb CA, Nagy L, Boyer MI. Posttraumatic reconstruction in the hand. *Instr Course Lect*. 2007;56:91-99.

20. Kunz M, Ma B, Rudan JF, Ellis RE, Pichora DR. Image-guided distal radius osteotomy using patient-specific instrument guides. *J Hand Surg Am*. 2013;38(8):1618-1624.

21. Leong NL, Buijze GA, Fu EC, Stockmans F, Jupiter JB; for Distal Radius Malunion Collaborative Group. Computer-assisted versus non-computer-assisted preoperative planning of corrective osteotomy for extra-articular distal radius malunions: a randomized controlled trial. *BMC Musculoskelet Disord*. 2010;11:282.

22. Lombardi AV Jr, Berend KR, Adams JB. Patient-specific approach in total knee arthroplasty. *Orthopedics*. 2008;31(9):927-930.

23. Meyer DC, Siebenrock KA, Schiele B, Gerber C. A new methodology for the planning of single-cut corrective osteotomies of mal-aligned long bones. *Clin Biomech (Bristol, Avon)*. 2005;20(2):223-227.

24. Miyake J, Murase T, Moritomo H, Sugamoto K, Yoshikawa H. Distal radius osteotomy with volar locking plates based on computer simulation. *Clin Orthop Relat Res*. 2011;469(6):1766-1773.

25. Murase T, Oka K, Moritomo H, Goto A, Yoshikawa H, Sugamoto K. Three-dimensional corrective osteotomy of malunited fractures of the upper extremity with use of a computer simulation system. *J Bone Joint Surg Am*. 2008;90(11):2375-2389.

26. Nakamura R, Horii E, Tanaka Y, Imaeda T, Hayakawa N. Three-dimensional CT imaging for wrist disorders. *J Hand Surg Br*. 1989;14(1):53-58.

27. Ng VY, DeClaire JH, Berend KR, Gulick BC, Lombardi AV Jr. Improved accuracy of alignment with patient-specific positioning guides compared with manual instrumentation in TKA. *Clin Orthop Relat Res*. 2012;470(1):99-107.

28. Oka K, Moritomo H, Goto A, Sugamoto K, Yoshikawa H, Murase T. Corrective osteotomy for malunited intra-articular fracture of the distal radius using a custom-made surgical guide based on three-dimensional computer simulation: case report. *J Hand Surg Am*. 2008;33(6):835-840.

29. Omori S, Murase T, Oka K, et al. Postoperative accuracy analysis of three-dimensional corrective osteotomy for cubitus varus deformity with a custom-made surgical guide based on computer simulation. *J Shoulder Elbow Surg*. 2015;24(2):242-249.

30. Potenza V, De Luna V, Maglione P, Garro L, Farsetti P, Caterini R. Post-traumatic malunion of the proximal phalanx of the finger. Medium-term results in 24 cases treated by "in situ" osteotomy. *Open Orthop J*. 2012;6:468-472.

31. Raaijmaakers M, Gelaude F, De Smedt K, Clijmans T, Dille J, Mulier M. A custom-made guide-wire positioning device for hip surface replacement arthroplasty: description and first results. *BMC Musculoskelet Disord*. 2010;11:161.

32. Radermacher K, Portheine F, Anton M, et al. Computer assisted orthopaedic surgery with image based individual templates. *Clin Orthop Relat Res*. 1998;(354):28-38.

33. Royle SG. Rotational deformity following metacarpal fracture. *J Hand Surg Br*. 1990;15(1):124-125.

34. Sarment DP, Sukovic P, Clinthorne N. Accuracy of implant placement with a stereolithographic surgical guide. *Int J Oral Maxillofac Implants*. 2003;18(4):571-577.

35. Schneider P, Eberly DH. *Geometric Tools for Computer Graphics*. San Francisco, CA: Morgan Kaufmann; 2002.
36. Schweizer A, Furnstahl P, Harders M, Szekely G, Nagy L. Complex radius shaft malunion: osteotomy with computer-assisted planning. *Hand*. 2010;5(2):171-178.
37. Schweizer A, Fürnstahl P, Harders M, Szekely G, Nagy L. Complex radius shaft malunion: osteotomy with computer-assisted planning. *Hand*. 2010;5(2):171-178.
38. Schweizer A, Fürnstahl P, Nagy L. Three-dimensional correction of distal radius intra-articular malunions using patient-specific drill guides. *J Hand Surg Am*. 2013;38(12): 2339-2347.
39. Schweizer A, Mauler F, Vlachopoulos L, Nagy L, Furnstahl P. Computer-assisted 3-dimensional reconstructions of scaphoid fractures and nonunions with and without the use of patient-specific guides: early clinical outcomes and postoperative assessments of reconstruction accuracy. *J Hand Surg Am*. 2016;41(1):59-69.
40. Trumble T, Gilbert M. In situ osteotomy for extra-articular malunion of the proximal phalanx. *J Hand Surg Am*. 1998;23(5):821-826.
41. Victor J, Premanathan A. Virtual 3D planning and patient specific surgical guides for osteotomies around the knee: a feasibility and proof-of-concept study. *Bone Joint J*. 2013;95-B(Suppl 11A):153-158.
42. Vlachopoulos L, Schweizer A, Graf M, Nagy L, Fürnstahl P. Three-dimensional postoperative accuracy of extra-articular forearm osteotomies using CT-scan based patient-specific surgical guides. *BMC Musculoskelet Disord*. 2015;16:336.
43. Vroemen JC, Dobbe JG, Strackee SD, Streekstra GJ. Positioning evaluation of corrective osteotomy for the malunited radius: 3-D CT versus 2-D radiographs. *Orthopedics*. 2013;36(2):e193-e199.
44. Weckesser EC. Rotational osteotomy of the metacarpal for overlapping fingers. *J Bone Joint Surg Am*. 1965;47:751-756.
45. Wu G, van der Helm FC, Veeger HE, et al. ISB recommendation on definitions of joint coordinate systems of various joints for the reporting of human joint motion——part II: shoulder, elbow, wrist and hand. *J Biomech*. 2005;38(5):981-992.
46. Zhang X, Liu Z, Shao X, Wang L, Huang X, Zhu H. Palmar opening wedge osteotomy for malunion of fifth metacarpal neck fractures. *J Hand Surg Am*. 2013;38(12):2461-2465.